Heliyon 9 (2023) e13352

Contents lists available at ScienceDirect

Heliyon

journal homepage: www.cell.com/heliyon

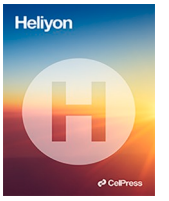

Research article

Transcriptomic analysis reveals the immune response of human microglia to a soy protein and collagen hybrid bioscaffold

Li Yao [a,*], Jacques Blasi [a], Teresa Shippy [b], Ryan Brice [a]

[a] Department of Biological Sciences, Wichita State University, 1845 Fairmount Street, Wichita, KS 67260, United States
[b] KSU Bioinformatics Center, Division of Biology, Kansas State University, Manhattan, KS 66506, United States

ARTICLE INFO

Keywords:
Microglia
Immune response
Soy protein
Bioscaffolds
Cell migration

ABSTRACT

Inflammatory reactions resulting from spinal cord injury cause significant secondary damage. Microglial cells activate $CD4^+$ T cells via major histocompatibility complex class II (MHCII) molecules. The activated T cells lead to neural tissue damage and demyelination at early stages of spinal cord injury. Control of the inflammatory response may attenuate the injury process. In this study, we compared gene expression in human microglia grown on soy protein-collagen hybrid scaffolds versus collagen scaffolds. Differentially expressed genes (DEGs) were subjected to gene ontology (GO) and pathway enrichment assays. Among down-regulated genes, the "antigen processing and presentation" pathway shows enrichment, primarily due to the down-regulation of MHCII molecules. The DEGs in this pathway show enrichment of binding sites for several transcription factors, with CIITA and IRF8 being the top candidates. The down-regulation of MHCII along with the significant enrichment of the GO term "focal adhesion" among the up-regulated genes helps explain the higher motility of microglial cells on the hybrid scaffold compared with that on the collagen scaffold. Up-regulated genes associated with "focal adhesion" include DNM2, AHNAK, and HYOU1, which have been previously implicated in increased cell motility. Overall, our study indicates that the use of hybrid scaffolds containing soy protein and collagen may modulate the immune response of wounded neural tissue.

1. Introduction

Soy protein has been recognized as a "green" and renewable material for tissue repair applications [1]. Various soy protein-based scaffolds have been generated and studied for cellular interaction and tissue repair. A previous study showed that electrospun soy protein nanofibers allow induced human pluripotent stem cells to properly differentiate into retinal pigment epithelium [2]. Moreover, freeze-dried porous soy protein scaffolds and bioscaffolds created by 3D printing with soy protein slurry support the growth of human mesenchymal stem cells [3,4].

In vivo studies have shown that scaffolds made from soy protein improve wound healing, in part by reducing inflammation. Spun nanofibers generated from cellulose acetate and soy protein hydrolysate were used to treat wounded mouse skin [5,6]. The grafts accelerated re-epithelialization and epidermal thinning during the healing process and reduced scarring [5]. Wound dressings made of electrospun soy protein nanofibers accelerated and enhanced skin regeneration after full thickness skin excision in a pig wound healing model [6]. A number of studies have tried to determine the molecular basis of the anti-inflammatory effect of soy protein. Most of the

* Corresponding author.
E-mail address: li.yao@wichita.edu (L. Yao).

https://doi.org/10.1016/j.heliyon.2023.e13352
Received 16 February 2022; Received in revised form 4 January 2023; Accepted 26 January 2023
Available online 1 February 2023

attention has been focused on estrogen-like compounds called isoflavones. One of the major soy isoflavones, genistein, reduces adhesion of monocytes to human vascular endothelial cells, and thus may be responsible for the protective effects of soy isoflavones against atherosclerosis [7]. Another study showed that genistein modulates the function of natural killer cells by reducing the production of interleukin (IL)-12/IL-18-induced interferon-gamma) [8].

Spinal cord injury (SCI) leads to an inflammatory response in neural tissue at the lesion site. The inflammatory reaction causes secondary damage and therefore control of this response may attenuate the injury process [9–11]. Several types of immune cells are involved in the inflammatory reaction. The resident immune cells, microglia, are activated a few minutes after SCI [12]. Other immune cells, including T cells, migrate and infiltrate the lesion, reaching peak amounts one week after the injury [13,14]. CD^{4+} T cells can be activated by microglia, which act as antigen-presenting cells via the major histocompatibility complex class II (MHCII) antigens on the microglial surface. The activated CD^{4+} T cells proliferate and differentiate into a few subtypes such as Th1, Th2, Th9, Th17 [15–17]. The activated T cells may cause further neural injury by secreting cytokines and activating other immune cells that exaggerate the injury [18–20]. Better functional recovery of wounded spinal cord was observed when T cells were suppressed [21–23].

In a previous study, we reported the creation of a multichannel conduit composed of soybean protein isolate (SPI) and collagen and characterized its chemical and mechanical properties. We also studied the growth of human microglial clone 3 cell line (HMC3) cells on the SPI-collagen composite scaffolds [24]. The conduit showed potential for neural repair applications. Although it has been shown that soy protein can reduce inflammatory reactions and contribute to wound healing in some tissues, it still not known if it can modulate the inflammatory function of immune cells in neural tissue. In this study, primary human microglia were grown on either SPI-collagen substrate or collagen substrate. RNA-Seq was performed to compare gene expression under the two conditions to determine whether soy protein-based scaffolds might affect inflammatory processes in microglia. A previous study suggested that the activation of T cells via MHCII antigens on dendritic cells requires antigen processing and regulation of cell motility [25,26]. These processes are coupled through the function of the major histocompatibility complex II–associated invariant chain (Ii/CD74), which is involved in antigen processing and also negatively regulates dendritic cell motility [25,26]. Investigation of MHCII gene expression and microglia migration on the hybrid bioscaffolds will help determine the effect of soy protein on the immunoregulatory function of microglia and the potential utility of soy protein-based bioscaffolds in regulating the immune response in damaged neural tissue.

2. Materials and methods

2.1. Motility assay of human microglial cells on SPI-collagen coated plates

To make the SPI-collagen scaffolds, a soybean protein isolate (SPI, MP Biomedicals, LLC, Santa Ana, CA) solution was generated as previously reported [24]. After SPI was added to distilled water (10% w/v), the mixture was stirred constantly while glycerol was added to the solution (weight ratio of glycerol to SPI: 50%). The solution was then heated at 55 °C for 30 min. Type I collagen solution was prepared by dissolving collagen sponge in acetic acid (10 mg/mL). The collagen solution and the cooled SPI solution were mixed at a protein weight ratio of 1:1.

Human brain microglial cells (Immortalized primary cells, Neuromics Inc, Minneapolis, MN) were cultured with Alpha-glia Expansion Medium containing 5% fetal bovine serum (FBS) (Neuromics Inc, Minneapolis, MN) in a 37 °C incubator with 5% CO_2. The SPI-collagen substrate was created in 24-well plates by spreading the SPI-collagen mixture (80 μl/well) in the wells and air-drying. Collagen coated dishes were prepared in the same way as a control. The dried membrane was crosslinked with 20 mM 1-ethyl-3-(3-dimethylaminopropyl) carbodiimide hydrochloride (EDC) and 20 mM N-hydroxysuccinimide (NHS). The crosslinked membrane was then washed with NaH_2PO_4 (0.1 M) and distilled water repeatedly. Before cell seeding, the membranes were washed with phosphate-buffered saline (PBS). To study cell migration, the human microglial cells were seeded in wells (50000/well) containing either SPI-collagen membrane or collagen membrane. After culturing for two days, the migration of microglial cells was documented with a Zeiss Axio Observer microscope. The environment of the microscope was controlled at 37 °C with CO_2 supply during imaging, which occurred every 2 min for 1 h. NIH ImageJ software was used to analyze cell migration distance and speed.

2.2. Next generation RNA sequencing

As described in Section 2.1, SPI-collagen or collagen membranes were created in 6-well plates by coating the wells with the appropriate solution followed by EDC and NHS crosslinking. Human microglial cells were seeded on the membranes at 200,000 cells per well. The microglial cells were cultured for 3 days and then RNA was extracted from the cultured cells with the Direct-zol RNA Microprep kit (Zymo Research, Irvine, CA).

RNA-Seq was performed at the Kansas University Medical Center Genome Sequencing Center. RNA libraries were prepared using the Universal Plus mRNA-Seq with NuQuant kit (Tecan Genomics 0520-A01). Libraries were validated using the D1000 ScreenTape Assay kit (Agilent Technologies 5067-5582) followed by concentration determination with a Qubit fluorometer. A concentration of 2.125 nM was used for multiplexed sequencing. Adapter ligation was verified by qPCR. The NovaSeq 6000 S1 Reagent Kit (200 cycle) (Illumina 20012864) was used to run the pooled libraries on an Illumina NovaSeq 6000 Sequencing System using 2 × 101 cycle sequencing with dual indexes. A one percent spike-in of PhIX Illumina Control library was included in the sequencing runs to allow measurement of error rates.

2.3. Data analysis of RNA gene sequencing assay

Paired reads from the RNA-Seq analysis were uploaded onto Beocat, the high-performance computing cluster at Kansas State University, for processing and analysis. Trimmomatic-0.39 [27] was used to remove adapter contamination and low-quality 3′ sequence (defined as a mean score of <15 in a four base window), after which Bowtie 2 [28] was used to align reads to a transcriptome extracted from the human genome (version GRCh38.p13) using the GCA_000001405.28_GRCh38.p13_genomic.gtf.gz annotation file [29]. Expression counts for each gene were determined using RSEM [30] and the probability of each gene being differentially expressed was calculated with EBSeq, which uses Bayesian statistics [31]. Differentially expressed genes were defined as the set of genes with a posterior probability of equivalent expression (PPEE) less than or equal to 0.05, which corresponds to a false discovery rate (FDR) of 5% [31].

Differentially expressed genes were separated into up-regulated and down-regulated gene sets using the Posterior Fold Change

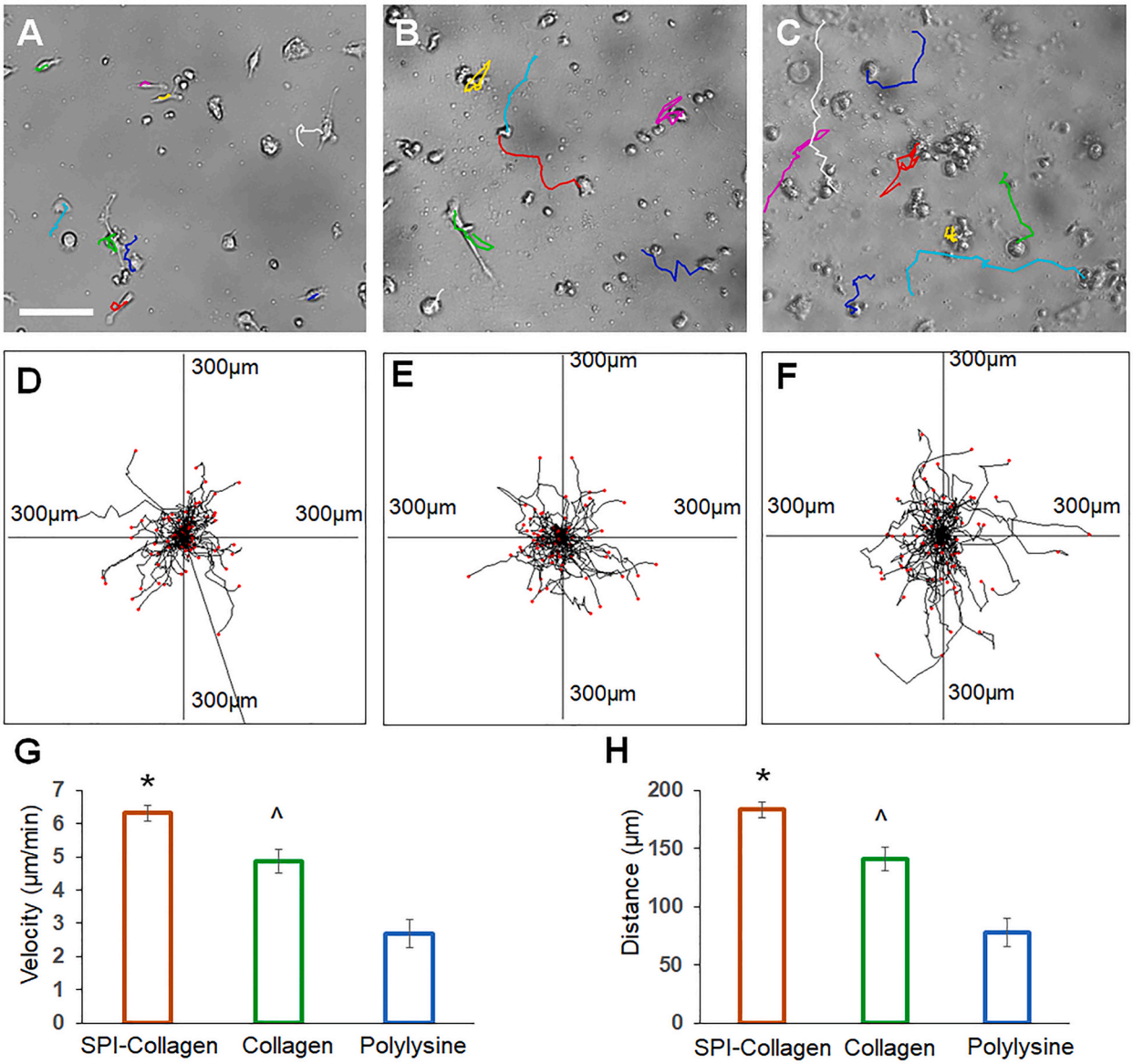

Fig. 1. Migration of human microglial cells. (A) Microglia migration on a polylysine-coated culture dish; (B) Microglia migration on a collagen treated culture dish; (C) Microglia migration on a SPI-collagen treated culture dish. Scale bar: 100 μm. Colored lines indicate individual cell migration tracks. (D–F) Graphs showing 1-h migration tracks of multiple microglial cells on polylysine (D), collagen (E) or SPI-collagen (F), with the starting position for each cell placed at the center of the graph. (G) Quantification of cell migration speed on different substrates; (H) Quantification of cell migration distance on different substrates. *, $p < 0.05$, vs. collagen and polylysine. ^, $p < 0.05$, vs. polylysine. Three independent replicates were performed in this study.

value calculated by EBSeq. These sets were analyzed using the Functional Annotation Tool from the Database for Annotation, Visualization, and Integrated Discovery (DAVID) [32,33] to identify enriched gene ontology terms and KEGG pathways [34]. GO terms or pathways with an adjusted p-value of less than 0.05 after use of the Benjamini-Hochberg correction for multiple testing were considered significantly enriched. The annotated KEGG pathway diagram was produced using Pathview [35]. DEGs associated with the "antigen processing and presentation" pathway were assessed for enrichment of transcription factor binding sites using ChEA3 [36] and Gene Set Enrichment Analysis (GSEA) Molecular Signatures Database (MSigDB) transcription factor target sets [37–40].

Normalized counts for up-regulated and down-regulated genes were used to create heatmaps with Heatmapper [41]. Data was scaled by row and hierarchically clustered by row using the absolute value of the Pearson correlation coefficient as the distance method and Average Linkage as the clustering method.

2.4. Statistical analysis

We used one-way ANOVA in SPSS to compare the velocity and migration distance of cells grown on different substrates, with a *p*-value of 0.05 considered statistically significant. Measurements are given as the mean plus or minus the standard deviation.

3. Results

3.1. Human microglial cell motility on SPI-collagen substrate

Migration of microglial cells on SPI-collagen membrane or collagen membrane was analyzed by using time-lapse images to track cell movement. The migration pathways of individual human microglial cells on different substrates are shown by colored lines in Fig. 1A–C. Individual cell migration tracks were superimposed on graphs in Fig. 1D–F. The center of each graph represents the initial position of all tracks. The tracks show the migration distance of the cells on different substrates. Quantitative analysis shows that the cell migration speed on SPI-collagen substrate is 6.3 ± 0.2 μm/min, which is significantly higher than the speed on collagen substrate (4.8 ± 0.3 μm/min, $p < 0.05$) (Fig. 1G). The migration distance of microglial cells on SPI-collagen membrane (183.4 ± 6.7 μm) is also significantly higher than that on collagen membrane (140.8 ± 10.5 μm, $p < 0.05$) (Fig. 1H). Supplemental videos 1, 2 and 3 show microglial cell migration on a polylysine-coated dish, collagen substrate, and SPI-collagen substrate, respectively.

3.2. GO term and KEGG analysis of differentially expressed genes

We performed RNA-Seq on three samples each of microglia grown on SPI-collagen or collagen substrate (Table 1). Differential expression analysis identified 149 up-regulated and 93 down-regulated genes in the cells grown on SPI-collagen substrate compared with those grown on collagen substrate (Fig. 2). We analyzed the up-regulated and down-regulated differentially expressed genes (DEGs) separately using the DAVID Functional Annotation Tool to identify significantly enriched GO terms and KEGG pathways for each gene set.

The analysis of down-regulated DEGs identified several significantly enriched GO terms that are related to the regulation of T cells (Fig. 3A). These GO terms include "MHC class II protein complex binding" and "MHC class II receptor activity" in the Molecular Function (MF) category and "antigen processing and presentation of peptide or polysaccharide antigen via MHC class II", "antigen processing and presentation", "antigen processing and presentation of exogenous peptide antigen via MHC class II", "T cell receptor signaling pathway", "T cell costimulation", and "T-helper 1 type immune response" in the Biological Process (BP) category.

For the up-regulated DEGs, the significantly enriched GO terms included "focal adhesion" (Fig. 3B). This GO term was associated with 13 DEGs (Table 2) including AHNAK nucleoprotein, calpain 2 (CAPN2), calreticulin (CALR), dynamin 2 (DNM2), heat shock protein family A (Hsp70) member 1B (HSPA1B), heat shock protein family A (Hsp70) member 5 (HSPA5), hypoxia up-regulated 1 (HYOU1), insulin like growth factor 2 receptor (IGF2R), peptidylprolyl isomerase B (PPIB), plectin (PLEC), prolyl 4-hydroxylase subunit beta (P4HB), scavenger receptor class B member 2 (SCARB2), and vimentin (VIM).

KEGG pathway enrichment analysis revealed 24 pathways enriched among down-regulated genes (Fig. 4A) and one pathway enriched among up-regulated genes (Fig. 4B). Many of the pathways enriched among down-regulated genes involve regulation of inflammatory reactions that could affect the inflammatory response of host to grafted scaffold, including "antigen processing and presentation" (13 DEGs) (Table 3 and Fig. 4C). Most of the DEGs in this set are MHCII genes, which is noteworthy because the

Table 1
RNA-Seq and mapping statistics for each sample. Mapped read pairs and alignment rate include all pairs that mapped at least once to the human GRCh38.p13 transcriptome.

Sample	Read pairs (raw)	Total bases (raw)	Read pairs (cleaned)	Total bases (cleaned)	Mapped read pairs	Alignment Rate
C1	39,420,244	7,884,048,800	38,681,240	7,739,643,114	32,351,292	83.64%
C2	32,059,797	6,411,959,400	31,436,195	6,290,578,302	26,185,720	83.30%
C3	34,057,891	6,811,578,200	33,410,006	6,685,667,039	27,957,625	83.68%
SPI1	32,232,744	6,446,548,800	31,611,246	6,324,944,069	26,298,194	83.19%
SPI2	31,909,770	6,381,954,000	31,321,324	6,274,199,109	26,179,472	83.58%
SPI3	28,040,493	5,608,098,600	27,470,000	5,495,223,238	22,800,287	83.00%

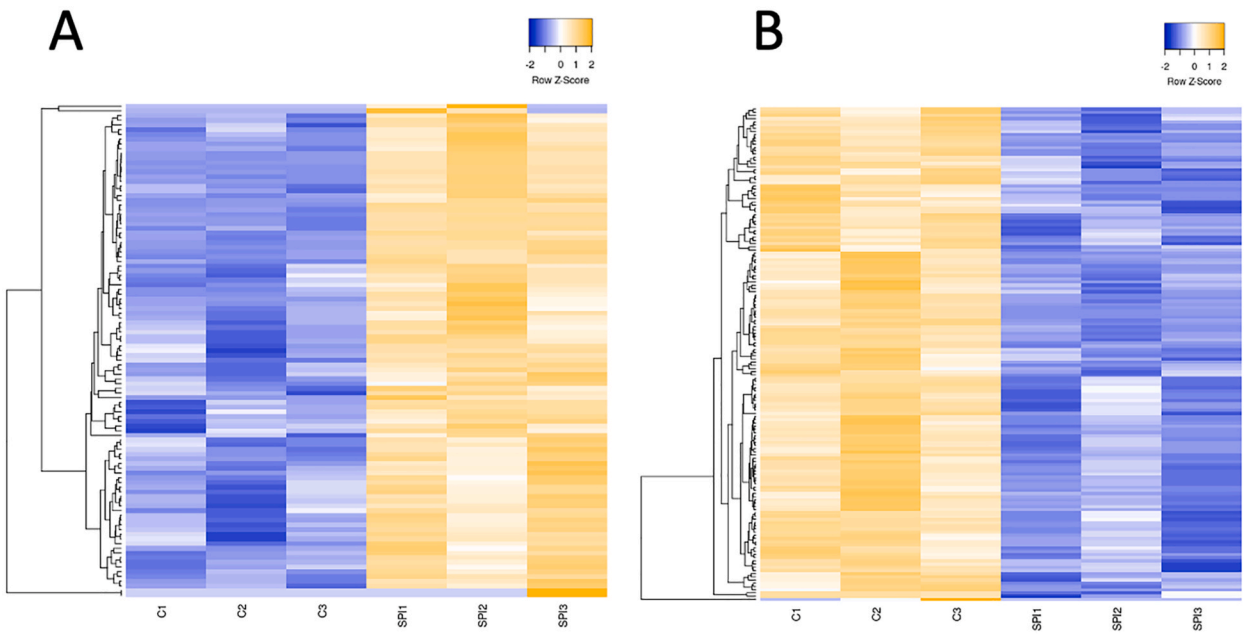

Fig. 2. Heatmaps of up-regulated (A) and down-regulated genes (B). Unsupervised hierarchical clustering (by row) of genes differentially expressed in microglia grown on SPI-collagen (SP1–SP3) versus on collagen (C1–C3) substrates. Rows represent genes and columns represent samples.

downregulation of MHCII molecules in microglial cells should decrease the activation of the $CD4^+$ T cells (Fig. 4C). The down regulation of MHCII may also contribute to the increased microglial motility on soy protein-collagen hybrid scaffolds [25,26,42]. Also of note, the enrichment of the "cell adhesion molecules (CAMs)" pathway (10 DEGs) among down-regulated genes could contribute to the increase in microglial motility on SPI-collagen substrate (Table 4) [42].

3.3. Transcription factor binding site enrichment for differentially expressed genes

Transcription factor (TF) binding site enrichment analysis was performed on the set of 13 DEGs in the "antigen processing and presentation" pathway, most of which are human leukocyte antigen (HLA) genes encoding MHCII molecules. Two different analysis tools using different sets of transcription factor data were used to investigate this gene set. GSEA MSigDB TF analysis shows that the gene set is significantly enriched in class II transactivator (CIITA) target genes. In the ChEA3 TF analysis, the top 10 TFs for the gene set are IRF8, NKX23, PAX5, IKZF3, RFX5, NFKB1, POU2AF1, IRF4, NFATC1, and BATF3. A local network of the top 10 TFs shows numerous connections between TFs (Fig. 5).

4. Discussion

In the central nervous system, microglia are a primary component of the innate immune system and are activated by spinal cord injury. This immune response contributes to functional recovery post SCI, but can also cause secondary damage. Numerous studies have reported the implantation of bioscaffolds after SCI to help regenerate wounded spinal cord. A neural conduit scaffold acts as a bridge to connect the gap across the neural defect and conduct axonal growth. In a previous study, we fabricated a soy protein and collagen hybrid protein scaffold and demonstrated that the scaffold supported the growth of hippocampal neurons, HMC3 cells and neural stem cells [24]. Other studies have suggested that soy protein may modulate the immune response in wounded tissue, because soy isoflavones regulate cytokine production and the function of immune cells [7,8,43]. However, it is not yet known how microglial cells respond to a scaffold containing soy protein. In this study, we compared gene expression in microglial cells grown on SPI-collagen substrate or collagen substrate to understand the effects of soy protein. Many of the DEGs with lower expression when grown on SPI-collagen are related to the immune function of microglial cells.

The "antigen processing and presentation" pathway, which is enriched among the down-regulated DEGs, is responsible for the interaction of microglial cells with CD^{4+} T cells. Most of the DEGs associated with this pathway are MHCII molecules. In fact, nine of the 15 MHCII genes show significantly reduced expression in microglia grown on SPI-collagen. Microglial cells activate $CD4^+$ T cells via MHCII molecules, so lower expression of MHCII genes could reduce T cell activation. Activated T cells lead to secondary neural tissue impairment and demyelination during early stages of SCI [23]. Subcutaneous injection of the immunosuppressant cyclosporin A in rats with spinal cord injury reduced T cell infiltration and microglia activation compared to untreated animals. The reduced immune cell response improved the preservation of residual myelination and the functional recovery of the wounded spinal cord [23]. Other studies showed that athymic nude rats lacking T cells had better locomotor function than normal rats after spinal cord injury,

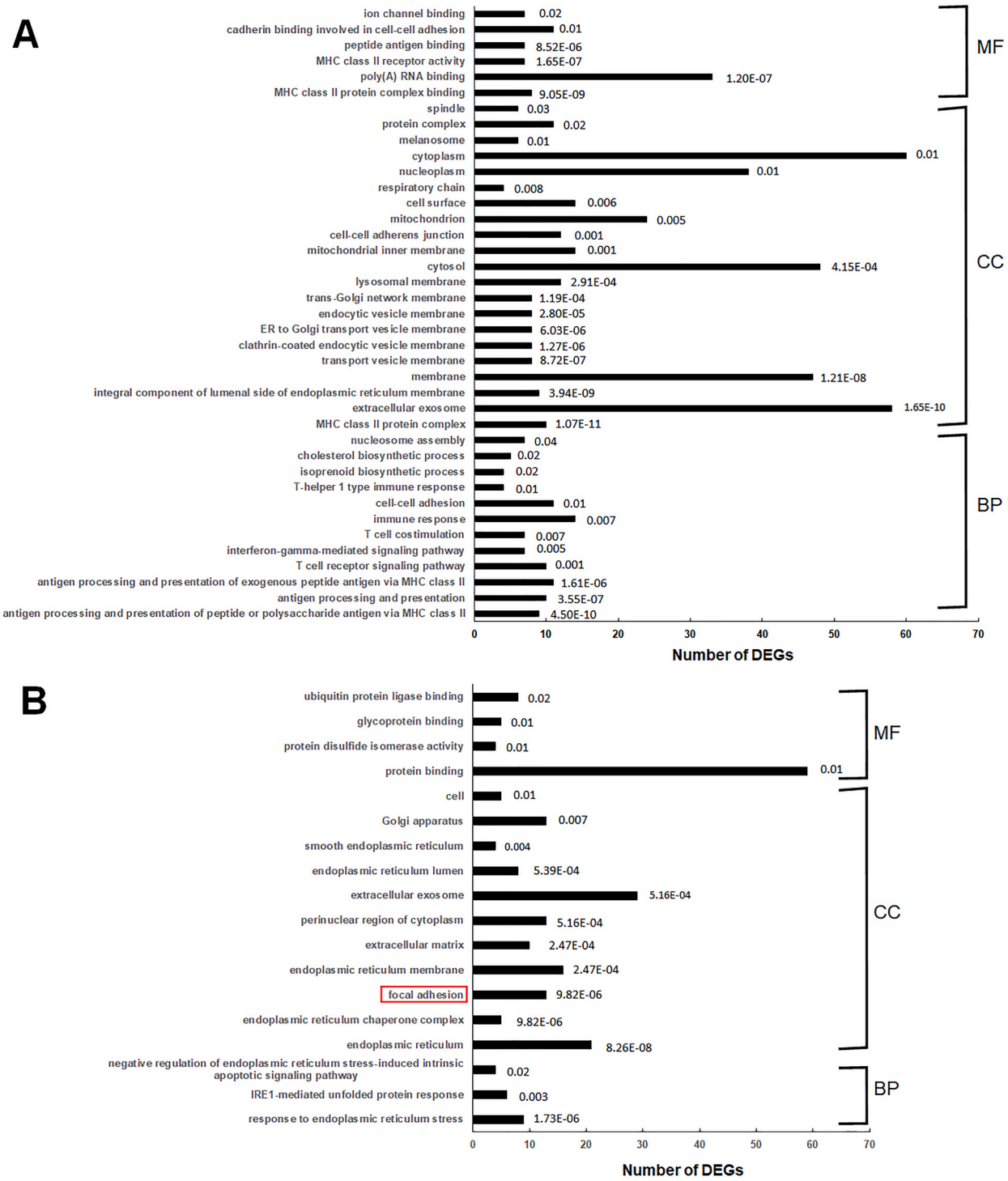

Fig. 3. GO term enrichment analysis. (A) Significantly enriched GO terms of down-regulated DEGs. (B) Significantly enriched GO terms of up-regulated DEGs. The significantly enriched GO term "focal adhesion" is highlighted.

particularly about a week after injury when T cell response would normally be greatest [21,44]. Our results suggest that use of an SPI-collagen scaffold may restrict the immune response induced by $CD4^+$ T cells and therefore attenuate the secondary injury to the spinal cord.

We were also interested in understanding the transcriptional control of the DEGs we identified. Transcription factors that regulate

Table 2
Genes associated with the enriched GO-CC term focal adhesion (adjusted p-value 1.7E-5) that are significantly upregulated in primary human microglia grown on SPI-collagen substrate. Posterior Probability of Equivalent Expression (PPEE) and Posterior Fold Change (PostFC) as calculated by EBSeq are shown for each differentially expressed gene. PPEE can be considered equivalent to the False Discovery Rate (FDR), with values less than 0.05 considered significant.

ENSEMBL_GENE_ID	Gene name	PPEE	PostFC
ENSG00000124942	AHNAK nucleoprotein (AHNAK)	0	0.58841176
ENSG00000138760	Scavenger receptor class B member 2(SCARB2)	0.00178483	0.74676144
ENSG00000204388	Heat shock protein family A (Hsp70) member 1B(HSPA1B)	0.02219659	0.79619198
ENSG00000162909	Calpain 2(CAPN2)	1.03E−07	0.84079051
ENSG00000178209	Plectin (PLEC)	8.57E−05	0.88409593
ENSG00000149428	Hypoxia up-regulated 1(HYOU1)	0	0.88428807
ENSG00000044574	Heat shock protein family A (Hsp70) member 5(HSPA5)	0	0.88508704
ENSG00000197081	Insulin like growth factor 2 receptor (IGF2R)	0.0004497	0.90423334
ENSG00000079805	Dynamin 2 (DNM2)	8.33E−05	0.91266271
ENSG00000026025	Vimentin (VIM)	2.27E−05	0.91673574
ENSG00000185624	Prolyl 4-hydroxylase subunit beta (P4HB)	0.00016091	0.92451871
ENSG00000166794	Peptidylprolyl isomerase B(PPIB)	6.59E−10	0.94477926
ENSG00000179218	Calreticulin (CALR)	1.16E−10	0.94812221

the function of microglia contribute to a number of neuropathological conditions [45,46]. We performed transcription factor binding site enrichment analysis of the DEGs to gain insight into the proteins that might be driving the differences in gene expression on the SPI-collagen substrate. In the GSEA MSigDB TF analysis of the 13 DEGs associated with the "antigen presentation and processing" KEGG pathway, we found that these genes are enriched in target sites for the CIITA transcription factor complex. This is not surprising since CIITA binds the transcription factors CREB, RFX and NF–Y to form an "enhanceosome" that is critical for expression of MHCII genes [47]. CIITA gene expression itself does not meet the criteria for statistically significant differential expression in our study, although it appears to be somewhat reduced in cells grown on SPI-collagen. Intriguingly, a previous study showed that treatment with an estrogen receptor beta (Erβ)-selective agonist reduced the expression of CIITA and consequently MHCII genes in microglia. When diarylpropionitrile was applied to cultured microglia or used to feed female mice, both CIITA and MHCII expression decreased, suggesting that ERβ-selective agonists could potentially treat multiple sclerosis by inhibiting MHCII expression in microglia [48]. Soy isoflavones are also ERβ-selective agonists, able to bind to estrogen receptors and regulate cell function [49,50]. Thus, it seems possible that the down-regulation of MHCII molecules we observed in microglial cells grown on SPI-collagen substrate could be at least partly caused by the effect of soy isoflavones on estrogen receptors. However, further study is needed to test this hypothesis.

ChEA3 analysis identified interferon regulatory factor 8 (IRF8) as the top-ranked TF associated with the DEGs in the "antigen presentation and processing" pathway as well as for the entire set of DEGs down-regulated on SPI-collagen. In microglia, IRF8 is required for the expression of genes that mediate microglial maturation, phagocytosis, and cytokine generation [51–53]. Importantly, IRF8 seems to be involved in development of reactive microglia. IRF8 expression was observed in spinal microglia after peripheral nerve injury. Moreover, *in vitro* overexpression of IRF8 in microglial cells resulted in the transcription of genes related to a reactive phenotype [52]. It has also been reported that IRF8 regulates microglial motility, with cell motility being notably reduced in the absence of IRF8 [51].

In vivo imaging of mouse neocortex has shown that resting microglial cells are very active and thus poised to respond to injury or disease [54]. After SCI, activated glial cells become more motile and are attracted to the lesion. Once there, microglia participate in the neuroprotective process by phagocytosis of dead and wounded neural tissue components [55]. In a lesion with a grafted conduit, cell motility along the surface of a grafted scaffold significantly affects the involvement of the microglia. We previously reported that the motility of HMC3 cells, a human microglial cell line, was not markedly different on SPI-collagen scaffold versus collagen scaffold [24]. In this work, we measured the motility of immortalized primary microglial cells on these substrates. In contrast to the previous study of HMC3 cells, we show that primary microglial cells are more motile on SPI-collagen substrate than on collagen substrate. Thus, grafting of SPI-collagen composite scaffolds into wounded spinal cord could enhance microglial cell migration toward the lesion and therefore facilitate microglial cell involvement in neural regeneration.

A previous study revealed the dual effect of MHCII molecules on antigen processing and cell motility of dendritic cells, with Ii-deficient cells showing increased cell motility [25]. Another study showed that MHCII genes must be downregulated to allow skin dendritic cell migration to lymph nodes [42]. In our study, we observed increased cell motility and reduced MHCII expression for microglia grown on SPI-collagen hybrid scaffolds compared with collagen scaffolds. This result is consistent with previous observations and suggests that soy protein can modulate microglial motility by reducing MHCII expression. We also found that the Cellular Component (CC) GO term "focal adhesion" was enriched among DEGs up-regulated in cells grown on SPI-collagen. Many of the thirteen up-regulated DEGs associated with this GO term have effects on migration. Here we discuss three examples: dynamin 2 (DNM2), AHNAK nucleoprotein, and hypoxia up-regulated 1(HYOU1). Dynamins, which are members of the large GTPase family, organize the polymerization of actin and regulate focal adhesion [56]. Overexpression of DNM2 in pancreatic ductal tumor cells led to increased cell migration velocity, while depletion of DNM2 significantly reduced cell migration [57]. AHNAK, a large structural protein also known as desmoyokin, has been implicated in migration and invasion in a variety of tumor cell types [58–61]. Knockdown of AHNAK in mesothelioma cell lines significantly decreased tumor cell motility and invasion ability [61]. HYOU1 is a heat shock protein 70 family member whose overexpression is associated with a poor prognosis in many cancer types. Silencing of HYOU1

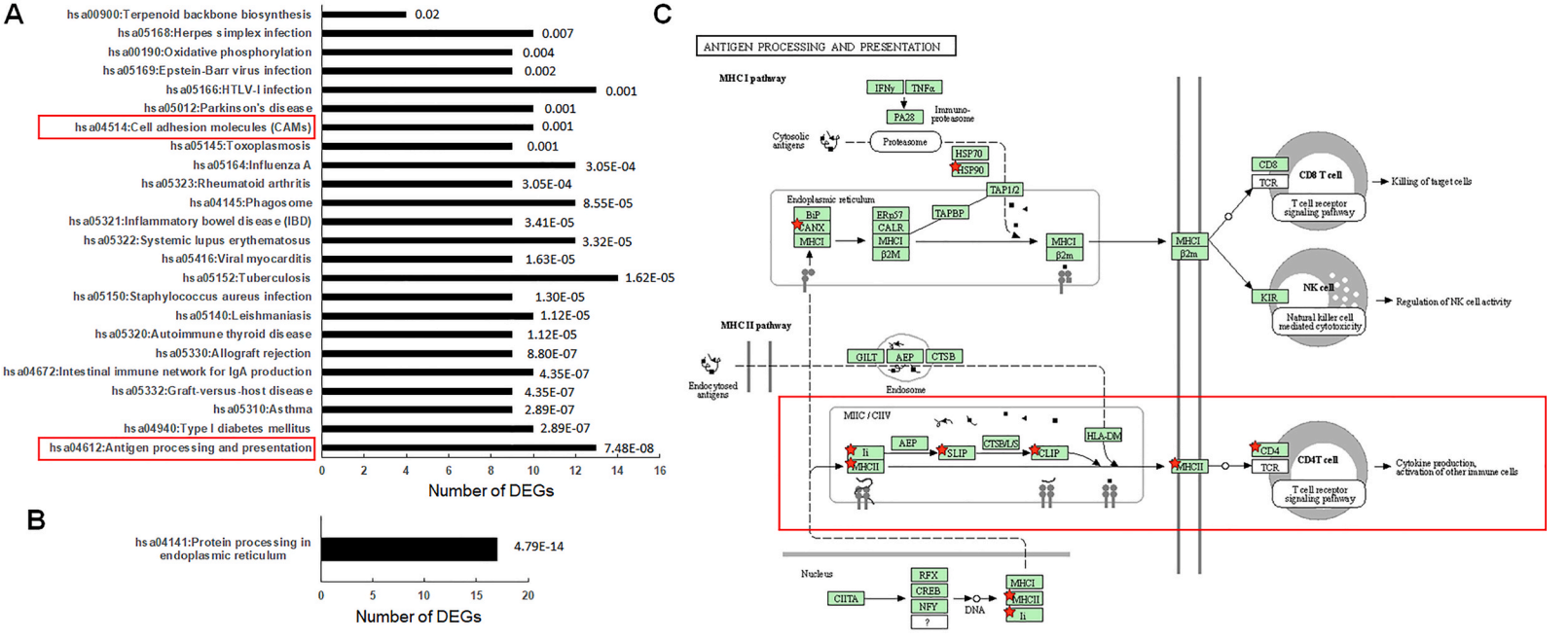

Fig. 4. KEGG pathway enrichment analysis of DEGs. (A) Pathways enriched among down-regulated DEGs. The antigen processing and presentation pathway is highlighted. (B) The single pathway enriched among up-regulated DEGs. (C) Diagram of the KEGG "antigen processing and presentation" pathway. Red stars indicate genes that are down-regulated in microglia grown on SPI-collagen. Note that the number of stars is not equal to the number of DEGs because some boxes (e.g. MHCII) represent multiple genes and others such as Ii, SLIP and CLIP are proteolytic products of a single protein. (For interpretation of the references to color in this figure legend, the reader is referred to the Web version of this article.)

Table 3
Genes associated with the enriched KEGG signaling pathway of antigen processing and presentation (adjusted p-value 8.1E-9) that are significantly down-regulated in primary human microglia grown on SPI-collagen substrate. Posterior Probability of Equivalent Expression (PPEE) and Posterior Fold Change (PostFC) as calculated by EBSeq are shown for each differentially expressed gene. PPEE can be considered equivalent to the False Discovery Rate (FDR), with values less than 0.05 considered significant.

ENSEMBL_GENE_ID	Gene name	PPEE	PostFC
ENSG00000096384	Heat shock protein 90 alpha family class B member 1(HSP90AB1)	0.0112477	1.03081833
ENSG00000127022	Calnexin (CANX)	1.46E−06	1.04324545
ENSG00000080824	Heat shock protein 90 alpha family class A member 1(HSP90AA1)	0.01249158	1.04476615
ENSG00000179344	major histocompatibility complex, class II, DQ beta 1(HLA-DQB1)	0.0153	1.08862569
ENSG00000196126	Major histocompatibility complex, class II, DR beta 1(HLA-DRB1)	0.00023991	1.09418428
ENSG00000019582	CD74 molecule (CD74)	8.83E−13	1.11870416
ENSG00000204252	Major histocompatibility complex, class II, DO alpha (HLA-DOA)	3.79E-05	1.13420614
ENSG00000196735	Major histocompatibility complex, class II, DQ alpha 1(HLA-DQA1)	2.22E−16	1.14140178
ENSG00000198502	major histocompatibility complex, class II, DR beta 5(HLA-DRB5)	0	1.15569127
ENSG00000231389	Major histocompatibility complex, class II, DP alpha 1(HLA-DPA1)	0	1.15923315
ENSG00000204287	Major histocompatibility complex, class II, DR alpha (HLA-DRA)	0	1.18760327
ENSG00000242574	Major histocompatibility complex, class II, DM beta (HLA-DMB)	3.77E−08	1.19366641
ENSG00000223865	Major histocompatibility complex, class II, DP beta 1(HLA-DPB1)	0	1.23255112

Table 4
Genes associated with the enriched KEGG signaling pathway of cell adhesion molecules (adjusted p-value 3.7E-4) that are significantly down-regulated in primary human microglia grown on SPI-collagen substrate. Posterior Probability of Equivalent Expression (PPEE) and Posterior Fold Change (PostFC) as calculated by EBSeq are shown for each differentially expressed gene. PPEE can be considered equivalent to the False Discovery Rate (FDR), with values less than 0.05 considered significant.

ENSEMBL_GENE_ID	Gene name	PPEE	PostFC
ENSG00000081237	protein tyrosine phosphatase, receptor type C(PTPRC)	0.00063544	1.07395023
ENSG00000179344	major histocompatibility complex, class II, DQ beta 1(HLA-DQB1)	0.0153	1.08862569
ENSG00000196126	major histocompatibility complex, class II, DR beta 1(HLA-DRB1)	0.00023991	1.09418428
ENSG00000204252	major histocompatibility complex, class II, DO alpha (HLA-DOA)	3.79E−05	1.13420614
ENSG00000196735	major histocompatibility complex, class II, DQ alpha 1(HLA-DQA1)	2.22E−16	1.14140178
ENSG00000198502	major histocompatibility complex, class II, DR beta 5(HLA-DRB5)	0	1.15569127
ENSG00000231389	major histocompatibility complex, class II, DP alpha 1(HLA-DPA1)	0	1.15923315
ENSG00000204287	major histocompatibility complex, class II, DR alpha (HLA-DRA)	0	1.18760327
ENSG00000242574	major histocompatibility complex, class II, DM beta (HLA-DMB)	3.77E−08	1.19366641
ENSG00000223865	major histocompatibility complex, class II, DP beta 1(HLA-DPB1)	0	1.23255112

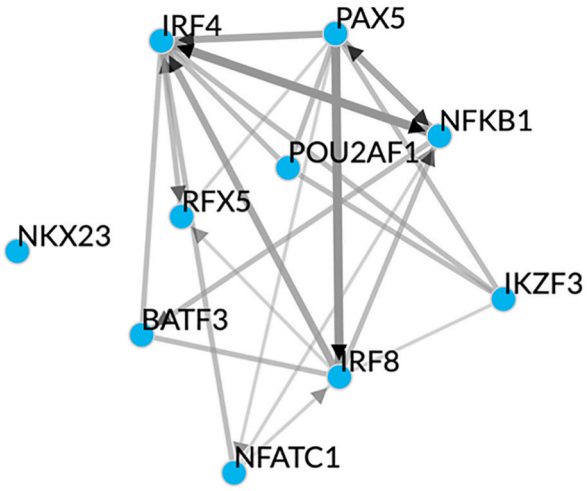

Fig. 5. Transcription factor binding site enrichment analysis with ChEA3. Local network clustering of the top 10 transcription factors whose binding sites are enriched in DEGs associated with the KEGG "antigen processing and presentation" pathway shows many interactions (either direct or indirect) among the enriched transcription factors. IRF8 and IRF4 appear to have the most interactions with other proteins suggesting they may be key drivers of differential expression for this gene set.

suppressed migration and invasion in epithelial ovarian cancer and papillary thyroid cancer cells [62,63].

5. Conclusion

In this study, we compared the response of human microglia to SPI-collagen and collagen substrates using RNA-Seq. We looked for enriched GO terms and pathways associated with genes differentially expressed during growth on the two materials. Association with the KEGG "antigen processing and presentation" pathway was enriched among genes downregulated on SPI-collagen. Interestingly, most of the DEGs in this set were MHCII genes. Previous studies have shown that MHCII molecules on the surface of microglial cells can activate $CD4^+$ T cells. The activated T cells can cause secondary neural tissue impairment and demyelination after spinal cord injury. Reduced expression of MHCII on the microglial surface may decrease T cell activation and attenuate the injury process. Transcription factor enrichment assays suggest that CIITA and IRF8 are likely regulators of the DEGs in the "antigen processing and presentation" gene set in response to the soy protein in the hybrid protein scaffold. We also found higher motility of microglia on the SPI-collagen substrate compared with that on collagen scaffold. The significantly enriched GO term focal adhesion is associated with 13 up-regulated genes, including DNM2, AHNAK, and HYOU1, that may mediate the higher motility of microglial cells on SPI-collagen substrate. This outcome indicates that microglia can migrate along SPI-collagen scaffolds to participate in the immune reaction after spinal cord injury. However, $CD4^+$ T cell activation by microglia may be reduced, perhaps limiting neural damage. Overall, our study indicates that the grafting of soy protein-collagen hybrid scaffolds may modulate the immune response of wounded neural tissue.

Author contribution statement

Li Yao: Conceived and designed the experiments; Performed the experiments; Analyzed and interpreted the data; Contributed reagents, materials, analysis tools or data; Wrote the paper.

Jacques Blasi, Ryan Brice: Performed the experiments; Analyzed and interpreted the data.

Teresa Shippy: Analyzed and interpreted the data; Contributed reagents, materials, analysis tools or data; Wrote the paper.

Funding statement

Teresa Shippy was supported by National Institute of General Medical Sciences [P20GM103418].

Li Yao was supported by John A. See Award from Wichita State University.

Data availability statement

Data included in article/supp. material/referenced in article.

Declaration of interest's statement

The authors declare that they have no known competing financial interests or personal relationships that could have appeared to influence the work reported in this paper.

Appendix A. Supplementary data

Supplementary data to this article can be found online at https://doi.org/10.1016/j.heliyon.2023.e13352.

References

[1] H. Jahangirian, S. Azizi, R. Rafiee-Moghaddam, B. Baratvand, T.J. Webster, Status of plant protein-based green scaffolds for regenerative medicine applications, Biomolecules 9 (10) (2019).

[2] M.A. Phelan, K. Kruczek, J.H. Wilson, M.J. Brooks, C.T. Drinnan, F. Regent, et al., Soy protein nanofiber scaffolds for uniform maturation of human induced pluripotent stem cell-derived retinal pigment epithelium. Tissue engineering Part C, Methods 26 (8) (2020) 433–446.

[3] K.B. Chien, R.N. Shah, Novel soy protein scaffolds for tissue regeneration: material characterization and interaction with human mesenchymal stem cells, Acta Biomater. 8 (2) (2012) 694–703.

[4] K.B. Chien, E. Makridakis, R.N. Shah, Three-dimensional printing of soy protein scaffolds for tissue regeneration. Tissue engineering Part C, Methods 19 (6) (2013) 417–426.

[5] S. Ahn, C.O. Chantre, A.R. Gannon, Lind JU, P.H. Campbell, T. Grevesse, et al., Soy protein/cellulose nanofiber scaffolds mimicking skin extracellular matrix for enhanced wound healing, Adv. Healthcare Mater. 7 (9) (2018), e1701175.

[6] Y-e Har-el, J.A. Gerstenhaber, R. Brodsky, R.B. Huneke, P.I.J.W.M. Lelkes, Electrospun Soy Protein Scaffolds as Wound Dressings: Enhanced Reepithelialization in a Porcine Model of Wound Healing, 2014, pp. 9–15, 5.

[7] B.K. Chacko, R.T. Chandler, A. Mundhekar, N. Khoo, H.M. Pruitt, D.F. Kucik, et al., Revealing anti-inflammatory mechanisms of soy isoflavones by flow: modulation of leukocyte-endothelial cell interactions, Am. J. Physiol. Heart Circ. Physiol. 289 (2) (2005) H908–H915.

[8] T.A. Mace, M.B. Ware, S.A. King, S. Loftus, M.R. Farren, E. McMichael, et al., Soy isoflavones and their metabolites modulate cytokine-induced natural killer cell function, Sci. Rep. 9 (1) (2019) 5068.

[9] J.C. Fleming, M.D. Norenberg, D.A. Ramsay, G.A. Dekaban, A.E. Marcillo, A.D. Saenz, et al., The cellular inflammatory response in human spinal cords after injury, Brain : J. Neurol. 129 (Pt 12) (2006) 3249–3269.

[10] E.D. Hall, The neuroprotective pharmacology of methylprednisolone, J. Neurosurg. 76 (1) (1992) 13–22.
[11] J.R. Bethea, Spinal cord injury-induced inflammation: a dual-edged sword, Prog. Brain Res. 128 (2000) 33–42.
[12] P.G. Popovich, Z. Guan, V. McGaughy, L. Fisher, W.F. Hickey, D.M. Basso, The neuropathological and behavioral consequences of intraspinal microglial/macrophage activation, J. Neuropathol. Exp. Neurol. 61 (7) (2002) 623–633.
[13] P.G. Popovich, P. Wei, B.T. Stokes, Cellular inflammatory response after spinal cord injury in Sprague-Dawley and Lewis rats, J. Comp. Neurol. 377 (3) (1997) 443–464.
[14] J.M. Sroga, T.B. Jones, K.A. Kigerl, V.M. McGaughy, P.G. Popovich, Rats and mice exhibit distinct inflammatory reactions after spinal cord injury, J. Comp. Neurol. 462 (2) (2003) 223–240.
[15] R. Putatunda, J.R. Bethea, W.H. Hu, Potential immunotherapies for traumatic brain and spinal cord injury, Chin. J. Traumatol. = Zhonghua chuang shang za zhi. 21 (3) (2018) 125–136.
[16] Y. Kumamoto, L.M. Mattei, S. Sellers, G.W. Payne, A. Iwasaki, CD4+ T cells support cytotoxic T lymphocyte priming by controlling lymph node input, Proc. Natl. Acad. Sci. U.S.A. 108 (21) (2011) 8749–8754.
[17] Y. Xiong, A. Mahmood, M. Chopp, Emerging potential of exosomes for treatment of traumatic brain injury, Neural Regener. Res. 12 (1) (2017) 19–22.
[18] M. Schroeter, S. Jander, T-cell cytokines in injury-induced neural damage and repair, Neuromol. Med. 7 (3) (2005) 183–195.
[19] E.N. Benveniste, Role of macrophages/microglia in multiple sclerosis and experimental allergic encephalomyelitis, J. Mol. Med. 75 (3) (1997) 165–173.
[20] D.P. Ankeny, K.M. Lucin, V.M. Sanders, V.M. McGaughy, P.G. Popovich, Spinal cord injury triggers systemic autoimmunity: evidence for chronic B lymphocyte activation and lupus-like autoantibody synthesis, J. Neurochem. 99 (4) (2006) 1073–1087.
[21] D. Satzer, C. Miller, J. Maxon, J. Voth, C. DiBartolomeo, R. Mahoney, et al., T cell deficiency in spinal cord injury: altered locomotor recovery and whole-genome transcriptional analysis, BMC Neurosci. 16 (2015) 74.
[22] A. Ibarra, D. Correa, K. Willms, M.T. Merchant, G. Guizar-Sahagún, I. Grijalva, et al., Effects of cyclosporin-A on immune response, tissue protection and motor function of rats subjected to spinal cord injury, Brain Res. 979 (1–2) (2003) 165–178.
[23] H.-Z. Lü, Y.-X. Wang, J.-S. Zhou, F.-C. Wang, J.-G. Hu, Cyclosporin A increases recovery after spinal cord injury but does not improve myelination by oligodendrocyte progenitor cell transplantation, BMC Neurosci. 11 (2010) 127.
[24] L. Yao, A. DeBrot, Fabrication and characterization of a protein composite conduit for neural regeneration, ACS Appl. Bio Mater. 2 (10) (2019) 4213–4221.
[25] G. Faure-André, P. Vargas, M.I. Yuseff, M. Heuzé, J. Diaz, D. Lankar, et al., Regulation of dendritic cell migration by CD74, the MHC class II-associated invariant chain, Science 322 (5908) (2008) 1705–1710.
[26] O. Leavy, Coordinating motility and function, Nat. Rev. Immunol. 9 (2) (2009) 73.
[27] A.M. Bolger, M. Lohse, B. Usadel, Trimmomatic: a flexible trimmer for Illumina sequence data, Bioinformatics 30 (15) (2014) 2114–2120.
[28] B. Langmead, S.L. Salzberg, Fast gapped-read alignment with Bowtie 2, Nat. Methods 9 (4) (2012) 357–359.
[29] V.A. Schneider, T. Graves-Lindsay, K. Howe, N. Bouk, H.C. Chen, P.A. Kitts, et al., Evaluation of GRCh38 and de novo haploid genome assemblies demonstrates the enduring quality of the reference assembly, Genome Res. 27 (5) (2017) 849–864.
[30] B. Li, C.N. Dewey, RSEM: accurate transcript quantification from RNA-Seq data with or without a reference genome, BMC Bioinf. 12 (2011) 323.
[31] N. Leng, Y. Li, B.E. McIntosh, B.K. Nguyen, B. Duffin, S. Tian, et al., EBSeq-HMM: a Bayesian approach for identifying gene-expression changes in ordered RNA-seq experiments, Bioinformatics 31 (16) (2015) 2614–2622.
[32] da W. Huang, B.T. Sherman, R.A. Lempicki, Bioinformatics enrichment tools: paths toward the comprehensive functional analysis of large gene lists, Nucleic Acids Res. 37 (1) (2009) 1–13.
[33] da W. Huang, B.T. Sherman, R.A. Lempicki, Systematic and integrative analysis of large gene lists using DAVID bioinformatics resources, Nat. Protoc. 4 (1) (2009) 44–57.
[34] M. Kanehisa, M. Furumichi, M. Tanabe, Y. Sato, K. Morishima, KEGG: new perspectives on genomes, pathways, diseases and drugs, Nucleic Acids Res. 45 (D1) (2017). D353-d61.
[35] W. Luo, G. Pant, Y.K. Bhavnasi, S.G. Blanchard Jr., C. Brouwer, Pathview Web: user friendly pathway visualization and data integration, Nucleic Acids Res. 45 (W1) (2017) W501–W508.
[36] A.B. Keenan, D. Torre, A. Lachmann, A.K. Leong, M.L. Wojciechowicz, V. Utti, et al., ChEA3: transcription factor enrichment analysis by orthogonal omics integration, Nucleic Acids Res. 47 (W1) (2019) W212–W224.
[37] A. Subramanian, P. Tamayo, V.K. Mootha, S. Mukherjee, B.L. Ebert, M.A. Gillette, et al., Gene set enrichment analysis: a knowledge-based approach for interpreting genome-wide expression profiles, Proc. Natl. Acad. Sci. U.S.A. 102 (43) (2005) 15545–15550.
[38] A. Liberzon, A. Subramanian, R. Pinchback, H. Thorvaldsdóttir, P. Tamayo, J.P. Mesirov, Molecular signatures database (MSigDB) 3.0, Bioinformatics 27 (12) (2011) 1739–1740.
[39] S. Kolmykov, I. Yevshin, M. Kulyashov, R. Sharipov, Y. Kondrakhin, V.J. Makeev, et al., GTRD: an integrated view of transcription regulation, Nucleic Acids Res. 49 (D1) (2020) D104–D111.
[40] X. Xie, J. Lu, E.J. Kulbokas, T.R. Golub, V. Mootha, K. Lindblad-Toh, et al., Systematic discovery of regulatory motifs in human promoters and 3′ UTRs by comparison of several mammals, Nature 434 (7031) (2005) 338–345.
[41] S. Babicki, D. Arndt, A. Marcu, Y. Liang, J.R. Grant, A. Maciejewski, et al., Heatmapper: web-enabled heat mapping for all, Nucleic Acids Res. 44 (W1) (2016) W147–W153.
[42] A. Majdoubi, J.S. Lee, M. Balood, A. Sabourin, A. DeMontigny, O.A. Kishta, et al., Downregulation of MHC Class II by Ubiquitination Is Required for the Migration of CD206+ Dendritic Cells to Skin-Draining Lymph Nodes, 2019, pp. 2887–2898, 203(11).
[43] M. Čoma, V. Lachová, P. Mitrengová, P. Gál, Molecular changes underlying genistein treatment of wound healing, Review 43 (1) (2021) 127–141.
[44] J.R. Potas, Y. Zheng, C. Moussa, M. Venn, C.A. Gorrie, C. Deng, et al., Augmented locomotor recovery after spinal cord injury in the athymic nude rat, J. Neurotrauma 23 (5) (2006) 660–673.
[45] V.H. Perry, J.A. Nicoll, C. Holmes, Microglia in neurodegenerative disease, Nat. Rev. Neurol. 6 (4) (2010) 193–201.
[46] I.R. Holtman, D. Skola, C.K. Glass, Transcriptional control of microglia phenotypes in health and disease, J. Clin. Invest. 127 (9) (2017) 3220–3229.
[47] D. Singer, B. Devaiah, CIITA and its Dual Roles in MHC Gene Transcription 4, 2013 (476).
[48] X. Liu, J. Deng, R. Li, C. Tan, H. Li, Z. Yang, et al., ERβ-selective agonist alleviates inflammation in a multiple sclerosis model via regulation of MHC II in microglia, Am. J. Tourism Res. 11 (7) (2019) 4411–4424.
[49] K.D. Setchell, Soy isoflavones–benefits and risks from nature's selective estrogen receptor modulators (SERMs), J. Am. Coll. Nutr. 20 (5 Suppl) (2001), 354S-62S; discussion 81S-83S.
[50] C.R. Cederroth, S. Nef, Soy, phytoestrogens and metabolism: a review, Mol. Cell. Endocrinol. 304 (1–2) (2009) 30–42.
[51] T. Masuda, N. Nishimoto, D. Tomiyama, T. Matsuda, H. Tozaki-Saitoh, T. Tamura, et al., IRF8 is a transcriptional determinant for microglial motility, Purinergic Signal. 10 (3) (2014) 515–521.
[52] T. Masuda, M. Tsuda, R. Yoshinaga, H. Tozaki-Saitoh, K. Ozato, T. Tamura, et al., IRF8 is a critical transcription factor for transforming microglia into a reactive phenotype, Cell Rep. 1 (4) (2012) 334–340.
[53] M. Horiuchi, K. Wakayama, A. Itoh, K. Kawai, D. Pleasure, K. Ozato, et al., Interferon regulatory factor 8/interferon consensus sequence binding protein is a critical transcription factor for the physiological phenotype of microglia, J. Neuroinflammation 9 (2012) 227.
[54] A. Nimmerjahn, F. Kirchhoff, F. Helmchen, Resting microglial cells are highly dynamic surveillants of brain parenchyma in vivo, Science 308 (5726) (2005) 1314–1318.
[55] E.A. Kolos, D.E. Korzhevskii, Spinal cord microglia in health and disease, Acta naturae 12 (1) (2020) 4–17.
[56] E. Lee, P. De Camilli, Dynamin at actin tails, Proc. Natl. Acad. Sci. U.S.A. 99 (1) (2002) 161–166.
[57] R.D. Eppinga, E.W. Krueger, S.G. Weller, L. Zhang, H. Cao, M.A. McNiven, Increased expression of the large GTPase dynamin 2 potentiates metastatic migration and invasion of pancreatic ductal carcinoma, Oncogene 31 (10) (2012) 1228–1241.

[58] J. Shankar, A. Messenberg, J. Chan, T.M. Underhill, L.J. Foster, I.R. Nabi, Pseudopodial actin dynamics control epithelial-mesenchymal transition in metastatic cancer cells, Cancer Res. 70 (9) (2010) 3780–3790.
[59] M. Sohn, S. Shin, J.-Y. Yoo, Y. Goh, I.H. Lee, Y.S. Bae, Ahnak promotes tumor metastasis through transforming growth factor-β-mediated epithelial-mesenchymal transition, Sci. Rep. 8 (1) (2018), 14379.
[60] F. Cheng, C. Liu, C.C. Lin, J. Zhao, P. Jia, W.H. Li, et al., A gene gravity model for the evolution of cancer genomes: a study of 3,000 cancer genomes across 9 cancer types, PLoS Comput. Biol. 11 (9) (2015), e1004497.
[61] H. Sudo, A.B. Tsuji, A. Sugyo, M. Abe, O. Hino, T. Saga, AHNAK is highly expressed and plays a key role in cell migration and invasion in mesothelioma, Int. J. Oncol. 44 (2) (2014) 530–538.
[62] X. Li, N.X. Zhang, H.Y. Ye, P.P. Song, W. Chang, L. Chen, et al., HYOU1 promotes cell growth and metastasis via activating PI3K/AKT signaling in epithelial ovarian cancer and predicts poor prognosis, Eur. Rev. Med. Pharmacol. Sci. 23 (10) (2019) 4126–4135.
[63] J.M. Wang, J.Y. Jiang, D.L. Zhang, X. Du, T. Wu, Z.X. Du, HYOU1 facilitates proliferation, invasion and glycolysis of papillary thyroid cancer via stabilizing LDHB mRNA, J. Cell Mol. Med. 25 (10) (2021) 4814–4825.